

# Hypnosis regulation in propofol anaesthesia employing super-twisting sliding mode control to compensate variability dynamics

ISSN 1751-8849  
 Received on 8th September 2018  
 Revised 9th May 2019  
 Accepted on 17th September 2019  
 E-First on 24th December 2019  
 doi: 10.1049/iet-syb.2018.5080  
 www.ietdl.org

Muhammad Ilyas<sup>1</sup>, Jamshed Iqbal<sup>2,3</sup> ✉, Sayyar Ahmad<sup>4</sup>, Ali Arshad Uppal<sup>1</sup>, Waqas Ahmad Imtiaz<sup>5</sup>, Raja Ali Riaz<sup>1</sup>

<sup>1</sup>Department of Electrical and Computer Engineering, COMSATS University, Islamabad, Pakistan

<sup>2</sup>University of Jeddah, College of Engineering, Department of Electrical and Electronic Engineering, Jeddah, Saudi Arabia

<sup>3</sup>Department of Electrical Engineering, FAST National University, Islamabad, Pakistan

<sup>4</sup>Department of Electrical Engineering, Cecos University of IT and Emerging Sciences, Peshawar, Pakistan

<sup>5</sup>Department of Electrical Engineering, Jalozai Campus, University of Engineering and Technology, Peshawar, Pakistan

✉ E-mail: jmiqbal@uj.edu.sa

**Abstract:** Regulation of hypnosis level on bi-spectral index monitor (BIS) during a surgical procedure in propofol anaesthesia administration is a challenging task for an anaesthesiologist in multi-tasking environment of the operation theater. Automation in anaesthesia has the potential to solve issues arising from manual administration. Automation in anaesthesia is based on developing the three-compartmental model including pharmacokinetics and pharmacodynamic of the silico patients. This study focuses on regulation of the hypnosis level in the presence of surgical stimulus including skin incision, surgical diathermy and laryngoscopy as well as inter-patient variability by designing super-twisting sliding mode control (STSMC). The depth of the hypnosis level is maintained to 50 on the BIS level in the maintenance phase after improving the induction phase to 60 s using the conventional sliding mode control and 30 s with STSMC. The proposed scheme also compensates the inter-patient variability dynamics including height, age and weight of the different silico patients. Moreover, the surgical stimuli direct the hypnosis level towards the state of consciousness and stimulate the controller to provide continuous drug infusion during the interval 80–90 s. Simulation results witness that the oscillatory behaviour is observed in drug infusion to ensure the moderate level of hypnosis (40–60) for general surgery.

## 1 Introduction

Surgical procedures are usually conducted with the induction of anaesthetics to achieve three basic objectives: hypnosis, analgesia and areflexia. The desired objectives can be achieved through an appropriate infusion of drugs to create the sensation of unconsciousness, lack of pain and lack of body movement. In the past inhaled gases like ether were applied to carry out the surgery to ensure safe and fast execution of procedure [1]. This method resulted in the high death rate due to complications in the anaesthesia procedure. As reported in [2], 150 people die every year in the USA. Crawford Williamson used diethyl ether to execute the first anaesthetic-based surgical procedure by introducing and realising the sensation of insensitiveness against pain [2]. The overall functional procedure of anaesthesia administration during surgery can be categorised into three phases including the induction, maintenance and emergence phases of anaesthesia. In the primary phase, the anaesthetics are administered to bring the patient to the desired hypnosis level, which is 50 on bi-spectral index monitor (BIS). The maintenance phase is a secondary phase where the desired hypnosis level is maintained so as to perform the surgery. The emergence phase is the last phase, which includes skin closure and brings the patient towards the awake state [3, 4].

Propofol is a hypnotic agent that consists of major ingredients of anaesthesia having a fast metabolism and no side effects to the patient. Appropriate infusion of propofol is obligatory to rely completely on the experience of an anaesthesiologist in manual

drug delivery administration. The overdosing and underdosing of propofol may, respectively, lead to severe consequences of cardiovascular collapse, or anxiety and trauma. Both of these conditions are unacceptable and intolerable to clinical professionals to ensure the safe execution of surgical procedures [5].

The advancement in the medical field has led us towards the development of well-equipped operation theaters for individuals to measure and control the unpredictable issues during the surgery to ensure highly trained and technical environment to minimise the human errors. For this reason, automation in anaesthesia is significant to develop sophisticated mechanisms by ensuring optimal delivery of drug infusion to regulate the hypnosis at a desirable scale [6, 7]. Schneider developed three compartmental models of silico patient including pharmacokinetics model (PK) shows the metabolism of a drug within body and pharmacodynamic (PD) indicate the effects of the drug on the depth of hypnosis (DoH) in the brain. The metabolism and distribution of drugs within the human body depend on age, height and weight of the body [8, 9]. The key functional component of anaesthesia is hypnosis, whose information is extracted from the cortical activity of the brain and is shown on the BIS monitor. Fig. 1 shows the scale of hypnosis level on the BIS monitor [10]. The DoH is scaled from 0 to 100 indicates the iso-electric EEG and complete awake state. The range 40–60 is the moderate band, in which surgical procedures are performed [10].

The BIS monitor is used to analyse the intra-operative awareness of patients during the surgery. The intra-operative awareness occurs due to the presence of pain during a surgical procedure as it can cause severe physiological consequences and can prolong the procedure. Based on surgical reviews conducted in the USA, the observed intra-operative awareness ranged between 0.2 and 1.6% [11, 12]. In the closed-loop control of anaesthesia administration, the BIS signal is used as a feedback signal to the controller [13]. To realise automation in anaesthesia, various

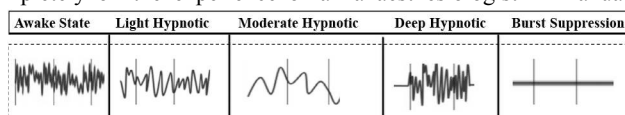


Fig. 1 DoH on BIS scale

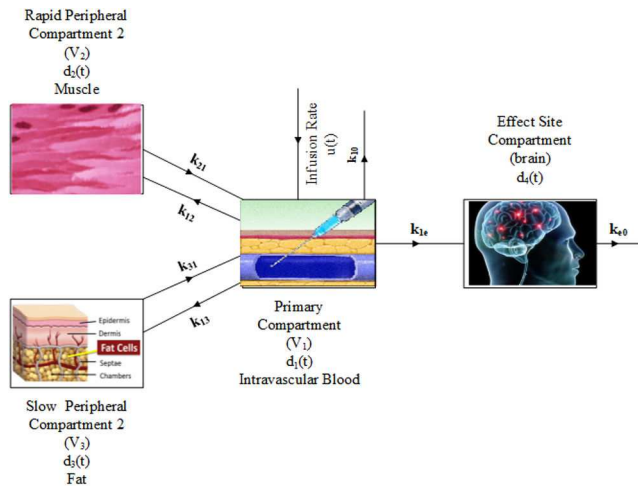


Fig. 2 Block diagram of PK and PD models

control strategies based on linear and non-linear controllers have been applied and investigated for different silico patients. Proportional integral derivative (PID) control is a classical technique with fast transient response applied by Chao Dong in 2003 [14]. In his work, he derived the three-compartmental model including the PK-PD model and linearised the output of the sigmoid model using linear regression. Moreover, he applied the PID control technique on hypothetical patients and achieved the desired results. However, a lot of data can be lost due to linear regression in the linearisation process [14]. Slotesz attempted to solve the problem by introducing the analgesic component of anaesthesia. As reported in [3, 15], he applied propofol and remifentanyl as hypnotic and analgesic components, respectively, and observed their synergetic effect. The major limitation of the Slotesz work is lack of handling inter-patient variability and intra-patient variability, which reduces the control performances and leads to instability of the system [16, 17]. Sliding mode control (SMC) is a non-linear control algorithm having robust behaviour towards higher order non-linear systems. SMC offers low sensitivity to plant structure variations and disturbances by moving the state trajectory towards the user-defined surface [18].

The non-linear dynamical system can be stabilised by applying the back-stepping control mechanism through the reduction of higher order system to low-order system in a recursive fashion. The major advantage of the back-stepping controller is its ability to handle the useful non-linearities of the system, but such mechanisms are not immune to structural variations and plant disturbances during the regulation of hypnosis in a closed-loop pattern [19]. The main challenges faced during the regulation of hypnosis to ensure safe surgery are inter-patient variability and intra-patient variability in automated anaesthesia infusion. Inter-patient variability refers to the variation of the patient dynamics like weight, height and age, which vary from patient to patient.

To address the challenges mentioned above to regulate the hypnosis level, robust control mechanisms can prove to be useful in terms of less sensitivity to perturbations like surgical stimuli occurred during the induction phase of anaesthesia infusion. The most considerable surgical stimulus is skin incision, which reduces the hypnosis level leading to awareness of the patient. One of the most prominent surgical stimuli is diathermy, in which high-frequency electromagnetic radiation is applied to coagulate the tissue by reducing the bleeding [20, 21].

Scientific literature reports various control algorithms for propofol anaesthesia administration. Model predictive control (MPC) is one such algorithm that can handle critical applications like anaesthesia control or glucose control. It can offer several features including BIS tracking and disturbance rejection capability. The performance of linear MPC is comparable with PID considering the time delay introduced by BIS monitor for anaesthesia control. However, the major limitation of the linear MPC is its inability to handle intra-variability dynamics like bleeding or hypnosis level variation due to skin incision. A predictive adaptive controller having the ability to monitor a

patient's responses continuously computes the drug level according to the specified BIS target. The regression model is then usually used for the prediction of a patient's response and to provide the adequate dosage level to keep the patient's hypnosis level in the desirable range. However, in the regression model, data can be lost especially due to linear regression [22, 23]. The present research based on super-twisting SMC (STSMC) considers all the limitations mentioned above and aims for promising results in terms of fast transient response and minimal steady-state error while handling parametric variations. A robust control strategy is developed to keep the hypnosis level between required bounds on BIS and to compensate various challenges related to inter-patient and intra-patient variabilities. The designed control strategy is based on a set of state equations derived from PK and PD models, which shows different responses of a patient to propofol infusion. STSMC is applied due to its less sensitivity towards patient parameters. The second advantage of STSMC is its robustness as compared to other control techniques such as MPC particularly in the presence of bleeding, which is a surgical stimulus. STSMC shows optimum results and removes the chattering in the hypnosis level on BIS. The performance of STSMC is investigated to achieve the desired hypnosis level during induction, maintenance and emergence phases of anaesthesia. The metabolism shown in results presents the plasma drug concentration in various compartments of the body based on three-compartmental PK-PD models. The controller input is analysed clinically for different silico patients. Intra-patient variability, which consists of surgical stimuli, is perturbation occurred during the surgery. It reduces the depth of anaesthesia and alters the consciousness of the patient thereby affecting skin incision, surgical diathermy and laryngoscopy. The model of the surgical stimulus is developed and the effects of stimuli on hypnosis during the closed-loop control of anaesthesia are investigated. The analytical analysis of STSMC is performed based on the Lyapunov theory. The performance achieved with the proposed control law is evaluated and analysed clinically considering all complications as well as limitations during the regulation of the hypnosis level in the presence of surgical stimuli. The rest of the paper is organised as follows: Section 2 describes the mathematical model of a patient based on the PK-PD model with all clinical parameters. Section 3 presents the proposed control methodology while Section 4 discusses the results achieved in different silico patients. Finally, Section 5 summarises the conclusion.

## 2 Compartmental model of the patient

Based on the flow of blood through various organs of the body at different rates, the overall human body can be divided into three compartments by proposing three-compartmental PK-PD model. Compartmental models describe all the basic approaches of drug metabolism, distribution and clearance as well as elimination in various organs of the body [24, 25]. Fig. 2 shows the three-compartmental PK-PD model with additional effect site compartment at the brain side of the human body.  $V_1$  shows the central compartment (intra-vascular blood) with rapid peripheral and slow peripheral compartments  $V_2$  and  $V_3$ , respectively. The distribution and metabolism of the drug among different compartments take place through weighted rate constants  $k_{12}$ ,  $k_{21}$ ,  $k_{13}$  and  $k_{31}$ , as shown in Fig. 2 [26]. The drug infusion is provided to the primary compartment containing the intra-vascular blood. The drug is then distributed to other compartments exponentially [3-7]. The output taken from the effect site compartment consists of cortical activity of the brain measured through BIS and scaled in terms of level.

To derive the PK model, state equations corresponding to the three compartments can be written as:

$$\dot{d}_1(t) = -k_{10}d_1(t) - k_{12}d_1(t) - k_{13}d_1(t) + k_{21}d_2(t) + k_{31}d_3(t) + u \quad (1)$$

$$\dot{d}_2(t) = k_{12}d_1(t) - k_{21}d_2(t) \quad (2)$$

$$\dot{d}_3(t) = k_{13}d_1(t) - k_{31}d_3(t) \quad (3)$$

**Table 1** State variables with description

State variables	Description	Unit
$d_1(t)$	amount of drug in primary compartment	mg
$d_2(t)$	amount of drug in rapid peripheral compartment	mg
$d_3(t)$	amount of drug in slow peripheral compartment	mg
$d_4(t)$	amount of drug in effect site compartment	mg
$u(t)$	drug infusion	mg/s

**Table 2** Sigmoid model parameters

Parameters	Description
$E_0$	shows fully awake stage without the infusion of a drug or a hypnotic agent
$E_{peak}$	effect achieved using a hypnotic agent
$C_{50}$	half of the maximum effect
$\gamma$	steepness or slope of the sigmoid curve

The PD model predicts the effect site concentration, as given by (4):

$$\dot{d}_4(t) = k_{1e}d_1(t) - k_{0e}d_4(t) \quad (4)$$

where  $k_{0e}$  and  $k_{1e}$  indicate the elimination rate constant and the weighted rate constant at effect site compartment, respectively.

The description of the above state variables given in (1)–(4) is given in Table 1.

The output of the infusion drugs is measured from the effect site compartment through non-linear sigmoid model on BIS which scales the consciousness level between 100 and 0 in (5):

$$BIS_{act} = E_0 - E_{peak} \times \frac{d_4^\gamma}{d_4 + C_{50}^\gamma} \quad (5)$$

The description of the sigmoid model parameters in (5) is given in Table 2.

Based on the patient's attributes, clinical parameters computed using the Schneider three-compartmental model for propofol are given in Table 3. Lean body mass (LBM) is a function of patient's gender, height and weight [25, 27].

### 2.1 Block diagram of open-loop anaesthesia infusion system

Fig. 3 presents the block diagram of the open-loop control of anaesthesia infusion system with step input  $u(t)$  cascaded with PK–PD model and sigmoid model.

### 2.2 Simulation results

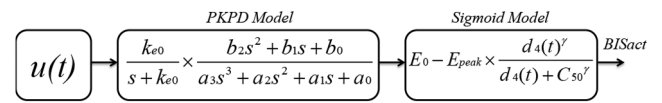
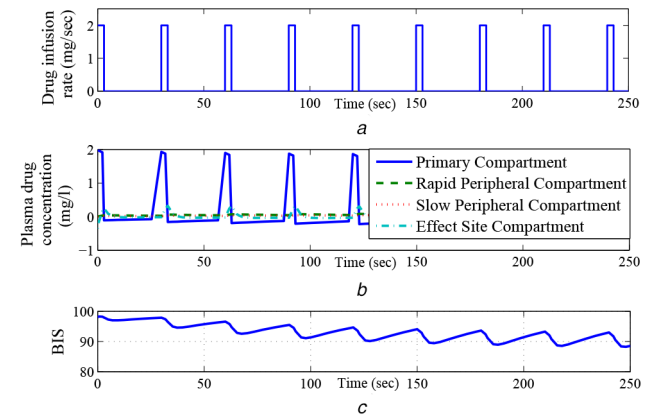
Fig. 4a shows the open-loop response or manual administration of propofol in the patient. The input drug infusion is provided in pulsating form with an amplitude of 2 mg/s and the period of pulse is 30 s and the duration of each pulse is 5 s. Fig. 4b shows the plasma drug concentration in various compartments of the body. The primary compartment is intra-vascular blood which acts as a carrier of the drug to different parts of the body including muscles, fats and brain. Fig. 4c shows the hypnosis level on BIS and the value of BIS is not uniform and the open-loop configuration is unable to achieve the desired DoH required for general surgery.

## 3 STSMC design

STSMC has been designed to maintain a desired BIS level. The design is carried out with and without surgical stimulus consisting of skin incision, surgical diathermy and laryngoscopy. The advantages of using STSMC are improved performance and chattering reduction as compared to other conventional SMC. Moreover, the STSMC retains the inherent robustness properties of

**Table 3** Clinical parameters of PK–PD model

Clinical parameters	Formula
LBM	male LBM = $1.1 \times W - 128 \times \frac{W^2}{H^2}$ female LBM = $1.07 \times W - 148 \times \frac{W^2}{H^2}$
weighted rate constants	$k_{10} = \frac{C_{L1}}{V_1}$ , $k_{13} = \frac{C_{L3}}{V_1}$ , $k_{21} = \frac{C_{L2}}{V_2}$ $k_{31} = \frac{C_{L3}}{V_3}$
volume of compartment	$V_1 = 4.27[l]$ $V_2 = 18.9 - 0.391(\text{Age} - 53)[l]$ $V_3 = 238[l]$
clearance	$C_{L1} = 1.89 + 0.0456(W - 77) - 0.0681(LBM - 59) + 0.0264(H - 177)$ $C_{L2} = 1.29 - 0.024(\text{Age} - 53)$ $C_{L3} = 0.836$

**Fig. 3** Open-loop control of propofol anaesthesia**Fig. 4** Open-loop administration of anaesthesia

SMC. In order to achieve the required performance, the following sliding surface is selected as [28–32]

$$\sigma = \dot{e} + n_1 e \quad (6)$$

$$e = BIS_{des} - BIS_{act} \quad (7)$$

where  $BIS_{des} = 50$  is the desired output for general surgery and  $n_1 \in \mathfrak{R}^+$  is a design parameter. The dynamics of the system under the ideal sliding mode ( $\sigma = 0$ ) is governed by

$$\sigma = \dot{e} + n_1 e = 0 \quad (8)$$

The above result implies that  $e(t)$  asymptotically converges to zero as

$$e(t) = e(0)e^{-n_1 t} \quad (9)$$

The control law is designed by taking the time derivative of (6):

$$\dot{\sigma} = \ddot{e} + n_1 \dot{e} \quad (10)$$

$$\dot{e} = 0 - E_{peak} \times \frac{d}{dt} \left( \frac{d_4(t)^\gamma}{d_4(t) + C_{50}^\gamma} \right) \quad (11)$$

$$\ddot{e} = \frac{E_{\text{peak}}\dot{d}_4\ddot{d}_4}{(K+d_4)^2} - \frac{2 \times E_{\text{peak}}\dot{d}_4^2\ddot{d}_4}{(K+d_4)^3} + \frac{2 \times E_{\text{peak}}\gamma d_4^{\gamma-1}\dot{d}_4^2}{(K+d_4)^2} - \frac{E_{\text{peak}}\gamma d_4^{\gamma-1}\dot{d}_4}{K+d_4} - (\gamma-1) \times \frac{E_{\text{peak}}\gamma d_4^{\gamma-2}\dot{d}_4^2}{K+d_4} \quad (12)$$

where  $K = C_{50}^{\gamma}$  and to ensure the finite-time convergence of sliding mode a super-twisting-based reachability law is selected as

$$\dot{\sigma} = -k_1 \left| \sigma \right|^{1/2} \text{sign}(\sigma) - k_2 \int \text{sign}(\sigma) d\tau \quad (13)$$

where  $k_1, k_2 \in \mathfrak{R}^+$  are controller gain parameters

$$k_1 \geq \frac{4\Phi\Psi_M(k_2 + \Phi)}{\Psi_m^2\Psi_m(k_2 - \Phi)}, \quad k_2 \geq \frac{\Phi}{\Psi_m} \quad (14)$$

The bounds of the gain parameter of sliding surface  $\Phi, \Psi$  are  $|\Phi| \leq \Phi$  and  $0 \leq \Psi_m \leq \Psi(\sigma, t) \leq \Psi_M$ , respectively, with  $\Phi, \Psi, \Psi_m$  and  $\Psi_M \in \mathfrak{R}^+$  [25]. Comparing the value of  $\dot{\sigma}$  from (10) and (13) to find the  $u$ :

$$\begin{aligned} -k_1 \left| \sigma \right|^{1/2} \text{sign}(\sigma) - k_2 \int \text{sign}(\sigma) d\tau &= \frac{E_{\text{peak}}\dot{d}_4\ddot{d}_4}{(K+d_4)^2} \\ &- \frac{2 \times E_{\text{peak}}\dot{d}_4^2\ddot{d}_4}{(K+d_4)^3} + \frac{2 \times E_{\text{peak}}\gamma d_4^{\gamma-1}\dot{d}_4^2}{(K+d_4)^2} - \frac{E_{\text{peak}}\gamma d_4^{\gamma-1}\dot{d}_4}{K+d_4} \\ &- (\gamma-1) \times \frac{E_{\text{peak}}\gamma d_4^{\gamma-2}\dot{d}_4^2}{K+d_4} + k_1 \dot{e} \end{aligned} \quad (15)$$

$$\begin{aligned} u &= \left[ \frac{2 \times E_{\text{peak}}\dot{d}_4\ddot{d}_4}{(K+d_4)^3} - \frac{2 \times E_{\text{peak}}\gamma d_4^{\gamma-1}\dot{d}_4^2}{(K+d_4)^2} + (\gamma-1) \right. \\ &\quad \left. \times \frac{E_{\text{peak}}\gamma d_4^{\gamma-2}\dot{d}_4^2}{K+d_4} - k_1 \dot{e} \right] \\ &\quad \times \frac{d_4(K+d_4)^2}{E_{\text{peak}}\dot{d}_4^{\gamma}(d_4(1-\gamma) - K\gamma)(-0.456\dot{d}_4 + 0.1068)} \\ &\quad + ((k_{10} + k_{12} + k_{13})d_1 - k_{21}d_2 - k_{31}d_3) \\ &\quad - k_1 \left| \sigma \right|^{1/2} \text{sign}(\sigma) - k_2 \int \text{sign}(\sigma) d\tau \end{aligned} \quad (16)$$

### 3.1 Existence of sliding mode

SMC algorithm is based on the non-linear stability theorem known as the Lyapunov stability theorem. In order to prove the stability of the control law designed, a suitable Lyapunov candidate function must be defined. The existence of the sliding mode can be proved by selecting the Lyapunov function, given as

$$\mathcal{V} = \frac{1}{2}\sigma^2 \quad (17)$$

If the derivative of the Lyapunov candidate function is always negative definite within the state space of the system, the system dynamics will converge to the desired set points. In order to prove that the control law designed will result in a negative definite first-order derivative of the Lyapunov function selected, the derivative of the Lyapunov function in (17) is stated below:

$$\dot{\mathcal{V}} = \sigma \dot{\sigma} \quad (18)$$

It is clear from (18) that the derivative of Lyapunov function consists of the first-order derivative of the sliding surface. The control law explicitly appears in the first derivative of the sliding surface, which is clear from the equation stated below:

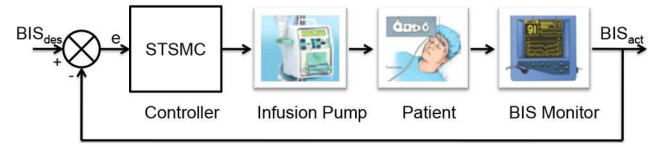


Fig. 5 Overall closed-loop system for anaesthesia infusion

$$\begin{aligned} \dot{\sigma} &= \left[ \frac{2 \times E_{\text{peak}}\dot{d}_4\ddot{d}_4}{(K+d_4)^3} - \frac{2 \times E_{\text{peak}}\gamma d_4^{\gamma-1}\dot{d}_4^2}{(K+d_4)^2} \right. \\ &\quad \left. + (\gamma-1) \times \frac{E_{\text{peak}}\gamma d_4^{\gamma-2}\dot{d}_4^2}{K+d_4} - k_1 \dot{e} \right] \\ &\quad \times \frac{d_4(K+d_4)^2}{E_{\text{peak}}\dot{d}_4^{\gamma}(d_4(1-\gamma) - K\gamma)(-0.456\dot{d}_4 + 0.1068)} \\ &\quad + ((k_{10} + k_{12} + k_{13})d_1 - k_{21}d_2 - k_{31}d_3) \\ &\quad - \left[ \frac{2 \times E_{\text{peak}}\dot{d}_4\ddot{d}_4}{(K+d_4)^3} - \frac{2 \times E_{\text{peak}}\gamma d_4^{\gamma-1}\dot{d}_4^2}{(K+d_4)^2} \right. \\ &\quad \left. + (\gamma-1) \times \frac{E_{\text{peak}}\gamma d_4^{\gamma-2}\dot{d}_4^2}{K+d_4} - k_1 \dot{e} \right] \\ &\quad \times \frac{d_4(K+d_4)^2}{E_{\text{peak}}\dot{d}_4^{\gamma}(d_4(1-\gamma) - K\gamma)(-0.456\dot{d}_4 + 0.1068)} \\ &\quad + ((k_{10} + k_{12} + k_{13})d_1 - k_{21}d_2 - k_{31}d_3) \\ &\quad - k_1 \left| \sigma \right|^{1/2} \text{sign}(\sigma) - k_2 \int \text{sign}(\sigma) d\tau \end{aligned} \quad (19)$$

Putting the value of  $\dot{\sigma}$  in (18):

$$\begin{aligned} \dot{\mathcal{V}} &= \sigma \left[ \frac{2 \times E_{\text{peak}}\dot{d}_4\ddot{d}_4}{(K+d_4)^3} - \frac{2 \times E_{\text{peak}}\gamma d_4^{\gamma-1}\dot{d}_4^2}{(K+d_4)^2} \right. \\ &\quad \left. + (\gamma-1) \times \frac{E_{\text{peak}}\gamma d_4^{\gamma-2}\dot{d}_4^2}{K+d_4} - k_1 \dot{e} \right] \\ &\quad \times \frac{d_4(K+d_4)^2}{E_{\text{peak}}\dot{d}_4^{\gamma}(d_4(1-\gamma) - K\gamma)(-0.456\dot{d}_4 + 0.1068)} \\ &\quad + ((k_{10} + k_{12} + k_{13})d_1 - k_{21}d_2 - k_{31}d_3) \\ &\quad - \left[ \frac{2 \times E_{\text{peak}}\dot{d}_4\ddot{d}_4}{(K+d_4)^3} - \frac{2 \times E_{\text{peak}}\gamma d_4^{\gamma-1}\dot{d}_4^2}{(K+d_4)^2} \right. \\ &\quad \left. + (\gamma-1) \times \frac{E_{\text{peak}}\gamma d_4^{\gamma-2}\dot{d}_4^2}{K+d_4} - k_1 \dot{e} \right] \\ &\quad \times \frac{d_4(K+d_4)^2}{E_{\text{peak}}\dot{d}_4^{\gamma}(d_4(1-\gamma) - K\gamma)(-0.456\dot{d}_4 + 0.1068)} \\ &\quad + ((k_{10} + k_{12} + k_{13})d_1 - k_{21}d_2 - k_{31}d_3) \\ &\quad - k_1 \left| \sigma \right|^{1/2} \text{sign}(\sigma) - k_2 \int \text{sign}(\sigma) d\tau \end{aligned} \quad (20)$$

$$\dot{\mathcal{V}} = -k_1 \left| \sigma \right|^{1/2} \text{sign}(\sigma) - k_2 \sigma \int \text{sign}(\sigma) d\tau \quad (21)$$

$$\dot{\mathcal{V}} = -k_1 \left| \sigma \right| \times \left| \sigma \right|^{1/2} - k_2 \sigma \int \text{sign}(\sigma) d\tau \quad (22)$$

$$\dot{\mathcal{V}} = -k_1 \left| \sigma \right|^{3/2} - k_2 \sigma \int \text{sign}(\sigma) d\tau \quad (23)$$

The system will be stable if  $k_1, k_2 > 0$ .

The overall closed-loop system is shown in Fig. 5. The controller adjusts the hypnosis level on the BIS monitor by changing the drug infusion level. The BIS signal acts as a feedback signal, as shown in Fig. 5. The patient acts as a plant with sensors

**Table 4** Clinical data set of different patients

Patient	Age	Height, cm	Weight	Gender	$C_{50}$	$E_0$	$E_{peak}$	$\gamma$
1	40	163	54	F	6.33	98.80	94.10	2.24
2	36	163	50	F	6.76	98.60	86.00	4.29
3	34	172	58	F	4.95	96.20	96.80	1.84
4	28	164	60	M	4.93	94.70	85.30	2.46
5	37	187	75	M	8.02	92.00	104.00	2.10
6	42	179	78	M	4.82	91.80	77.90	1.85
7	38	174	80	F	6.56	95.50	76.40	4.12
8	43	163	59	F	12.10	90.20	147.00	2.42

**Table 5** Parameters analysis based on variance and standard deviation

Patient	Age	Mean	Variance	Standard deviation
1	40	37.25	18.87	4.343
2	36	—	—	—
3	34	—	—	—
4	28	—	—	—
5	37	—	—	—
6	42	—	—	—
7	38	—	—	—
8	43	—	—	—
patient	weight	—	—	—
1	54	64.25	118.18	10.87
2	50	—	—	—
3	58	—	—	—
4	60	—	—	—
5	75	—	—	—
6	78	—	—	—
7	80	—	—	—
8	59	—	—	—
patient	height	—	—	—
1	163	170.625	40.23	6.34
2	163	—	—	—
3	172	—	—	—
4	164	—	—	—
5	187	—	—	—
6	179	—	—	—
7	174	—	—	—
8	163	—	—	—

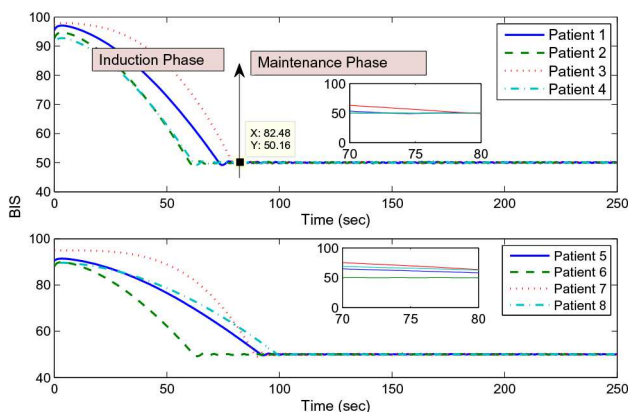
and surgical stimulus. The inter-patient variability compensation illustrates the controller ability to give optimum results in the case of changing the weight, height and age from patient to patient. Whether the surgical stimulus is the intra-patient variability depends on those variables which vary among the same patient during a surgical procedure.

#### 4.1 Inter-patient variability compensation with STSMC

Table 4 lists the clinical parameters of eight silico patients [33]. These patients have different attributes including age, height, weight and gender. The controller performance is monitored and observed for all these patients.

Table 5 shows the inter-patient variability analysis of different patients considering the variance and standard deviation. The variance and standard deviation are computed considering the different variables like age, height and weight of the patients. The desired hypnosis level of 50 is achieved using both conventional SMC- and STSMC-based laws, respectively, as shown in Figs. 6 and 7 by compensating the inter-patient variability. The standard deviation is 4.343, 10.87 and 6.34 in terms of age, weight and height of the patient, respectively, for different patients. The controller parameters are considered as nominal, which are not changing from patient to patient. Fig. 8 presents the drug distribution and metabolism in different compartments of the human body after infusion based on conventional SMC. Primarily drug is administered into the intra-vascular blood referred as a primary compartment, where it exponentially decays into other parts of the body including muscles, bones and brain. As the drug decays in the primary compartment of the body, it slowly rises in rapid and slow peripheral compartments exponentially. Oscillatory behaviour is observed due to variations in drug infusion so as to achieve the reference level of hypnosis. Figs. 9 and 10 show the controller drug infusion level for eight patients. The conventional SMC is applied to achieve the desired performances. The controller response demonstrates the transient state of 80 s and after achieving the desired hypnosis level, a steady-state response is initialised. The oscillatory behaviour observed in the steady state shows the controller response to handle the chattering and variation in the hypnosis level. Moreover, variations in (a–d) in Fig. 9 and (e–h) in Fig. 10 are observed due to the difference in age, height and weight of the first four patients. Patient 4 is younger compared to the other seven patients in Table 4 and hence shows rapid metabolism.

Fig. 6 shows the hypnosis level on BIS for all eight patients. Hypnosis level is divided into two phases: induction phase and maintenance phase. The induction phase achieved the reference level 50 on BIS in nearly 80 s and then the maintenance phase is initialised. All eight patients achieved the desired hypnosis level demonstrating the ability of the controller to handle inter-patient variability. As patient 4 is younger than the other seven patients, therefore he rapidly tunes to the desired hypnosis level without showing oscillations from the reference value of hypnosis on BIS. Younger the patient, faster is the metabolism of drugs within the human body as evident from the clearance second equation of Table 3.

**Fig. 6** Hypnosis level in induction and maintenance phase on BIS

consisting of electrodes on his/her skull measuring the cortical activity of the brain.

## 4 Results and discussion

The result achieved by the implementation of STSMC consists of two subsections including inter-patient variability compensation

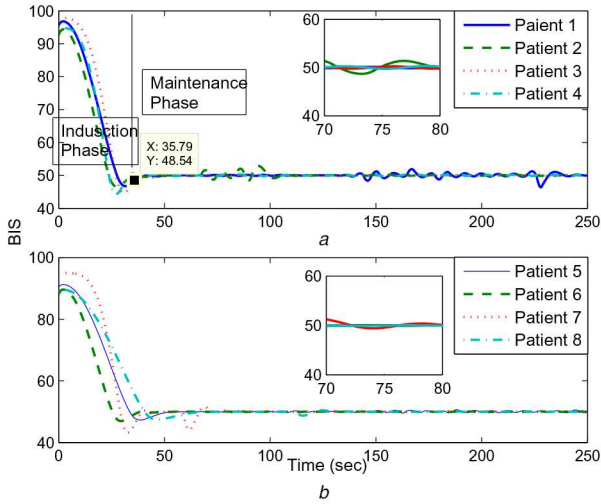


Fig. 7 Hypnosis level in induction and maintenance phase on BIS

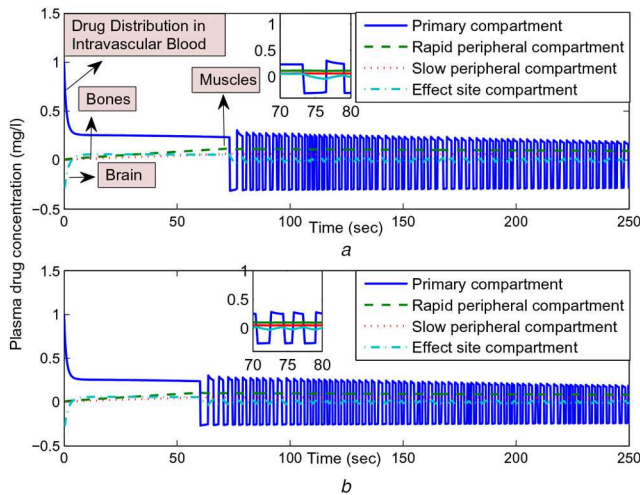


Fig. 8 Drug concentration in various compartments for (a) Patient 1, (b) Patient 2

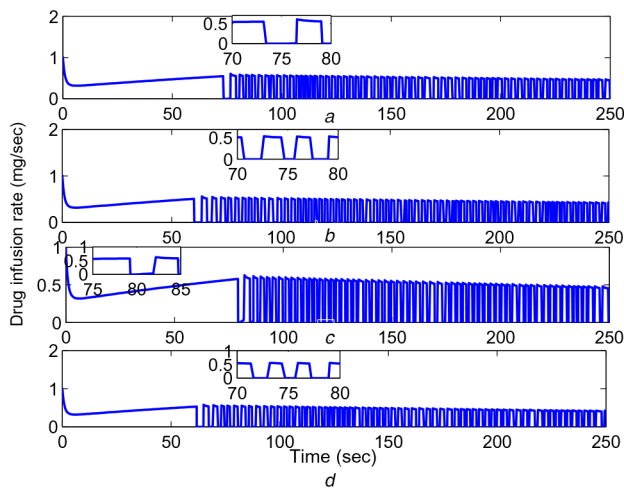


Fig. 9 Drug infusion level of (a) Patient 1, (b) Patient 2, (c) Patient 3, (d) Patient 4

#### 4.2 Inter-patient variability compensation with STSMC

Fig. 11 illustrates the plasma drug concentration for the first two patients in different organs of the body. The exponential decay of drug in the primary compartment of the body reflects the increment of drug in the remaining three compartments. The drug elimination and metabolism are smoothly occurred in STSMC system by reducing the sharp oscillatory behaviour of drug distribution observed in conventional SMC. Fig. 12 shows the drug infusion in

all eight patients with the application of STSMC. As previously discussed, the infusion level is classified into two sections: induction phase and maintenance phase. The induction phase is observed for nearly 30 s followed by the maintenance phase. The oscillatory behaviour is observed for all eight patients to compensate the chattering in the hypnosis level thereby ensuring robust behaviour. Primarily, the drug infusion is maximum in the transient phase to achieve the desired hypnotic level and later on minimal drug infusion is provided in the maintenance phase to maintain the desired level required for surgical procedure. Fig. 7 presents the hypnosis level on BIS scale marked from 0 to 100. It is observed that STSMC has a fast transient response that reduces it to 32 s as compared to 80 s observed previously in conventional SMC in Fig. 6. The rapid induction leads to the oscillation in the hypnosis level. Particularly, a deviation is observed in the case of patients 1, 2 and 7 which is within an acceptable range. Moreover, in the present case, the deviation from the reference value (50) is nearly 5% which ensures the compensation in inter-patient variability both in induction and maintenance phases as well. As it is clear from Fig. 7 that the hypnosis level is maintained between 40 and 60 on BIS which is required for the general surgical procedure. The controller provides different levels of drug infusion to patients of different age and weight.

#### 4.3 Surgical stimuli

The perturbation occurred during the surgery (called as surgical stimuli) reduces the depth of anaesthesia leads to awareness of the patient. The most prominent surgical stimuli are skin incision, surgical diathermy and laryngoscopy. Skin incision gets initialised after achieving the reference level of hypnosis on BIS thereby reducing the depth of anaesthesia [20, 21]. The surgical diathermy is applied to stop the bleeding of small blood vessels during the surgical procedure reducing the depth of anaesthesia in the form of hypnosis. Moreover, the laryngoscopy facilitates the breathing to ensure the oxygen saturation during surgery and prevents the trachea to be collapsed [34]. Fig. 13 shows the surgical stimuli modelled in (24), consists of piecewise defined function. Surgical stimuli mapped the three important physiological conditions mentioned above, which occur predominantly during procedures. In Fig. 7, point A represents the skin incision, which overshoots the BIS for an instant and thus reduces the hypnosis level, point B shows the laryngoscopy that is actually performed after the induction phase to facilitate the breathing and prevents the trachea to be collapsed. The third portion of stimuli is surgical diathermy, which is performed for coagulation of small blood vessels resulting in the reduction of the depth of anaesthesia by transduction of heat waves across the sensory neuron stimulates the hypnosis level towards the awareness state:

$$\text{surgical stimuli}(\Delta\text{BIS}) = \begin{cases} 0, & t < 80 \\ 15, & 80 \leq t \leq 81 \\ 10 \times e^{-0.1t}, & 81 < t \leq 140 \\ 7, & 140 < t \leq 160 \\ 0, & t > 160 \end{cases} \quad (24)$$

Now the output becomes  $\text{BIS}_{\text{act}} = E_0 - E_{\text{peak}} \times (d_4^t / (d_4 + C_{50}^t)) + \Delta\text{BIS}$ . The error function will also change due to surgical stimulus added in the output function. So (21) becomes

$$\dot{\sigma} = -k_1 |\sigma|^{2/3} - k_2 \sigma + \Delta\text{BIS} \quad (25)$$

The system will be stable if  $k_1, k_2 > 0$  and  $5 \leq \Delta\text{BIS} \leq 15$  are bounded. Fig. 14 presents the drug infusion level in the presence of surgical stimuli consisting of the induction phase and the maintenance phase. At point A, where the skin incision is occurs, the hypnosis level tends to direct towards the awake state which stimulates the controller to increase the infusion level by providing drugs continuously without any delay in the interval 80–90 s. Moreover, at point B, the surgical stimulus is reduced in terms of

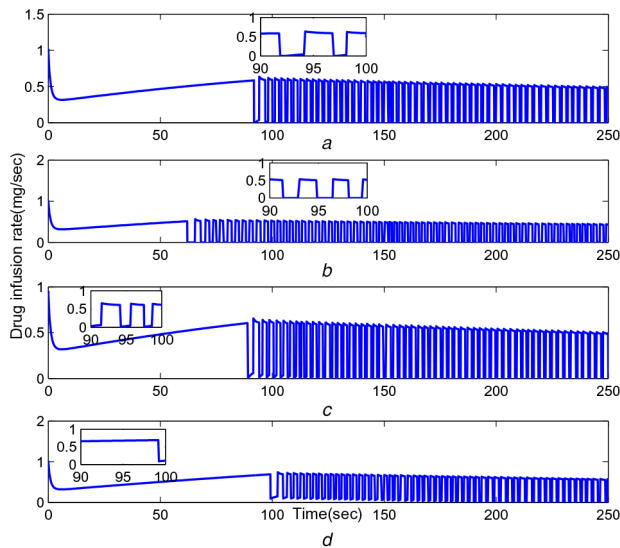


**Fig. 10** Drug infusion level of (a) Patient 5, (b) Patient 6, (c) Patient 7, (d) Patient 8

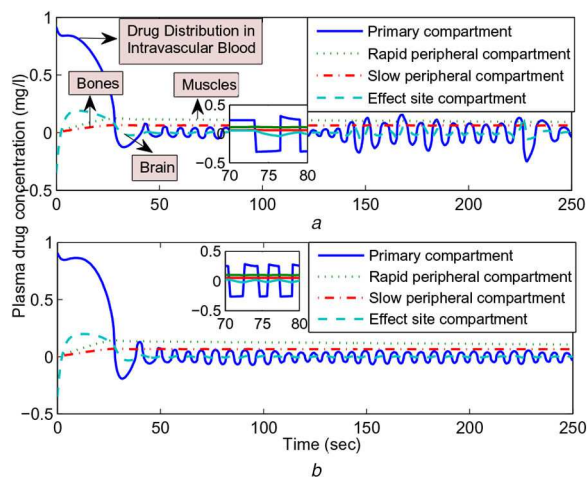


**Fig. 11** Plasma drug concentration in (a) Patient 1, (b) Patient 2

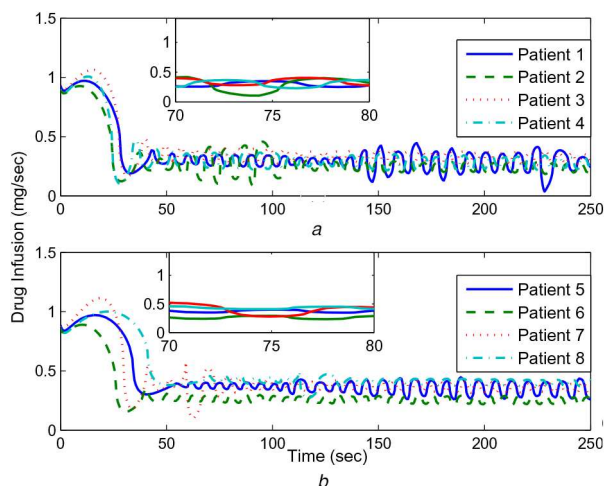


**Fig. 12** Controller drug infusion to the patients

laryngoscopy and the controller infusion level is provided in terms of pulses. At point C, the surgical diathermy is observed during the interval 140–160 s, which causes a reduction in the depth of anaesthesia stimulating the controller to initialise the increment operation in the infusion. At point D, the patient sensitivity is observed and the controller stops the infusion due to increment in the hypnosis level, as illustrated in Fig. 15. Fig. 15 shows the

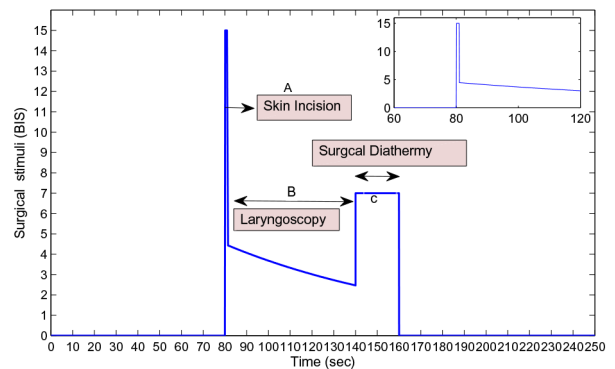


**Fig. 13** Surgical stimuli

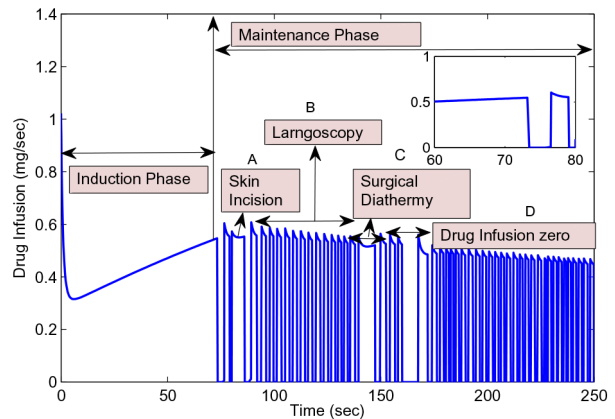


**Fig. 14** Drug infusion in presence of surgical stimuli

hypnosis level on BIS scaled from 0 to 100 in the presence of surgical stimuli in terms of all the three parameters. The effects of surgical stimulus get initialised during the maintenance phase of anaesthesia and show the maximum effect on the hypnosis level particularly during the skin incision. The controller responds quickly in Fig. 13 and achieves the reference level of hypnosis in <15 s during the general surgical procedure without any overshoot. All these features demonstrate the robust behaviour of the controller in the presence of surgical stimuli. Fig. 16 shows the tracking error ( $e$ ) between the desired BIS value and the actual BIS value. The tracking error is maximum during the induction phase of anaesthesia and later on, it reduces in the maintenance phase of anaesthesia. The variation in tracking error at various points is presented in Table 6. The performance error (PE) is also listed in Table 6.

Automation in anaesthesia faces a lot of challenges towards its applications on real patients. There is an increasing trend in the scientific community to address these challenges and limitations through the implementation of different control algorithms. The present research focuses to rectify the limitations by realising automation in anaesthesia based on a modern control algorithm. The simulated work shows optimum results considering parametric variations amongst the different patients and same patient as well. The compensation of inter-patient variability dynamics for different silico patients is obtained and investigated based on variance and standard deviation of those parameters including height, weight and age of the patients. The data set of eight patients with different clinical parameters is investigated and discussed based on the performance indices of the controller. It is evident from (23) that the proposed system is stable for  $k_1, k_2 > 0$ . The controller parameters are kept constant while the patient parameters are changing from patient to patient to ensure inter-patient variability. Perturbations occurred during the surgical procedure intervene the smooth conduction of surgery including skin incision, surgical diathermy and laryngoscopy. It is evident from the results that the transient response time is nearly 30 s with no overshoot being observed in settling time. The steady-state error is found to be <5%, which is clinically acceptable to maintain the DoH in the range of 40–60 for major surgery. Moreover, the

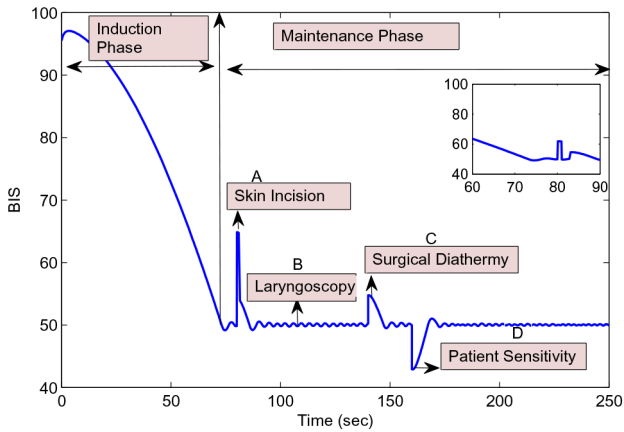


Fig. 15 BIS in presence of surgical stimuli

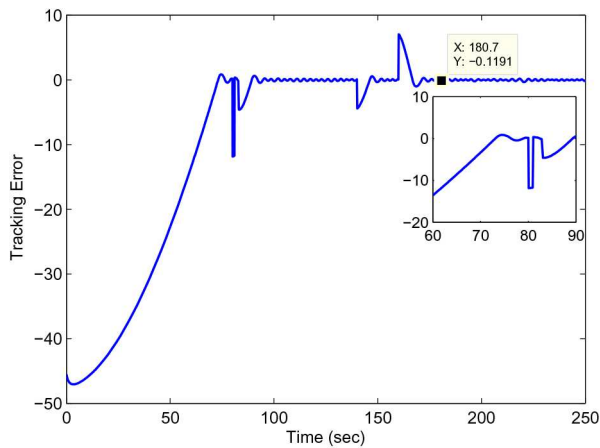


Fig. 16 Tracking error ( $e$ )

Table 6 Numeric values of tracking error ( $e$ ) and performance error (PE)

Time axis	$e = BIS_{des} - BIS_{act}$	$PE = \frac{BIS_{des} - BIS_{act}}{BIS_{des}}$
0	-45	-0.45
10	-46	-0.46
20	-42	-0.42
30	-37	-0.37
40	-30	-0.30
50	-20	-0.20
60	-13	-0.13
70	0.3	0.003
80	-11	-0.11
90	0.37	0.00017
100	-0.17	0.000815
110	-0.11	-0.002297
120	0.0029	0.00225
130	-0.168	-0.00336
140	0.01333	0.0002666
150	-0.075	-0.0015
160	0.055	0.0011
170	-0.299	-0.0598
180	-0.01191	-0.002382

plasma drug concentration profiles show the exponential decay of drug from intravascular blood to muscle and bones as well. The metabolism and distribution of the drug in various organs of the body indicate the tissue level flow of the drug in the human body. The results obtained from different aspects of the closed-loop control of anaesthetic infusion are clinically acceptable and are

consistent with the literature cited from current research in the field of health care and anaesthesiology.

## 5 Conclusions

This paper proposes a non-linear control law based on conventional SMC and STSMC algorithms for the regulation of hypnosis in propofol anaesthesia administration during a surgical procedure. The optimum level of hypnosis regulation between 40 and 60 is ensured in different patients by handling the inter-patient variability and compensating the surgical stimuli in terms of skin incision, surgical diathermy and laryngoscopy. The controller responds quickly to surgical stimuli and retains the reference value in <15 s. Automation in anaesthesia is the best solution for handling the major issues occurring during a surgical procedure in the operation theater.

The current research work is formulated for closed-loop control of anaesthesia based on the data set of healthy patients. The proposed scheme can be further strengthened by adding the dynamics of a diabetic patient to facilitate the surgical procedures for such patients. This can be done by integrating Bergman's model and three compartmental PK-PD model to automate anaesthesia for diabetic patients.

## 6 References

- [1] Stephane, B.: 'Automation in clinical anesthesia'. PhD thesis, University of British Columbia, 2006
- [2] Bibian, S., Ries, C.R., Huzmezan, M., *et al.*: 'Introduction to automated drug delivery in clinical anesthesia', *Eur. J. Control*, 2005, **11**, pp. 535–557
- [3] Soltesz, K.: 'Automation in anesthesia'. PhD thesis, Lund University, 2013
- [4] Padula, F., Ionescu, C., Latronico, N., *et al.*: 'Inversion-based propofol dosing for intravenous induction of hypnosis', *Commun. Nonlinear Sci. Numer. Simul.*, 2016, **39**, pp. 481–494
- [5] Warpechowski, P., dos Santos, A.T.L., Pereira, P.J.L., *et al.*: 'Effects of propofol on the cardiac conduction system', *Rev. Bras. Anesthesiol.*, 2010, **60**, pp. 441–444
- [6] Absalom, A.R., Sutcliffe, N., Kenny, G.N.: 'Closed-loop control of anaesthesia using bispectral index performance assessment in patients undergoing major orthopedic surgery under combined general and regional anaesthesia', *Anesthesiology*, 2002, **96**, (1), pp. 67–73
- [7] Absalom, A.R., Struys, M.M.R.F.: 'An overview of target controlled infusions and total intravenous anaesthesia' (Academia Press, San Diego, CA, USA)
- [8] Hendrickx, J.F.: 'The pharmacokinetics of inhaled anaesthetics and carrier gases'. PhD thesis, Ghent University, 2004
- [9] van Heusden, K., Dumont, G.A., Soltesz, K., *et al.*: 'Design and clinical evaluation of robust PID control of propofol anaesthesia in children', *IEEE Trans. Control Syst. Technol.*, 2014, **22**, pp. 491–501
- [10] Bibian, S., Dumont, G.A., Zikov, T.: 'Dynamic behavior of BIS, M-entropy and neuroSENSE brain function monitors', *J. Clin. Monit. Comput.*, 2011, **25**, pp. 81–87
- [11] Sebel, P.S., Bonke, B.E., Winograd, E.E.: 'Memory and awareness in anaesthesia'. Int. Symp. on Memory and Awareness in Anaesthesia, Atlanta, GA, USA, 1993
- [12] Domino, K.B., Posner, K.L., Caplan, R.A., *et al.*: 'Awareness during anaesthesia a closed claims analysis', *J. Am. Soc. Anesthesiologists*, 1999, **90**, pp. 1053–1061
- [13] Soltesz, K., Heusden, K.V., Hast, M., *et al.*: 'A synthesis method for automatic handling of inter-patient variability in closed-loop anaesthesia'. Proc. Int. Conf. IEEE American Control Conf., Boston, MA, USA, July 2014, pp. 4877–4882
- [14] Dong, C.: 'Closed-loop controlled total intravenous anaesthesia'. PhD thesis, University of Plymouth, 2003
- [15] Soltesz, K., Dumont, G.A., Ansermino, J.M.: 'Assessing control performance in closed-loop anaesthesia'. Proc. Int. Conf. 21st Mediterranean Conf. in Control & Automation, Chania, Greece, June 2013, pp. 191–196
- [16] Soltesz, K., Hahn, J.-O., Dumont, G.A., *et al.*: 'Assessing control performance in closed-loop anaesthesia'. Proc. Int. Conf. 21st Mediterranean Conf. in Control & Automation, Chania, Greece, June 2011, pp. 855–860
- [17] Bartkowska-Sniatkowska, A., Bienert, A., Wiczling, P., *et al.*: 'Pharmacokinetics and pharmacodynamics of propofol in children undergoing different types of surgeries', *Pharmacol. Rep.*, 2014, **66**, pp. 821–829
- [18] Huh, S.H., Bien, Z.: 'Robust sliding mode control of a robot manipulator based on variable structure-model reference adaptive control approach', *IET Control Theory Applic.*, 2007, **1**, (5), pp. 1355–1363
- [19] Liao, Y., Liao, F.: 'Design of a back-stepping tracking controller for a class of linear systems with actuator delay', *Math. Probl. Eng.*, 2015, **9**, pp. 1–10
- [20] Jordan, C., Weller, C., Thornton, C., *et al.*: 'Monitoring evoked potentials during surgery to assess the level of anaesthesia', *J. Med. Eng. Technol.*, 1995, **19**, pp. 77–79
- [21] Wilson, D.H.: 'The effects of pulsed electromagnetic energy on peripheral nerve regeneration', *Ann. New York Acad. Sci.*, 1974, **238**, pp. 575–585
- [22] Marrero, A., Mendez, J.A., Maslov, A.V., *et al.*: 'ACLAC: an approach for adaptive closed-loop anaesthesia control'. Proc. of the 26th IEEE Int. Symp. on Computer-Based Medical Systems, Porto, Portugal, 2013, pp. 285–290

- [23] Borera, E.C., Moore, B.L., Doufas, A.G., *et al.*: 'An adaptive neural network filter for improved patient state estimation in closed-loop anesthesia control'. 23rd Int. Conf. on Tools with Artificial Intelligence, Boca Raton, FL, USA, 2011, pp. 41–46
- [24] Shargel, L., Yu, A.: '*Applied biopharmaceutics & pharmacokinetics*' (McGraw-Hill company, USA, 2016, 7th edn.)
- [25] Schnider, T.W., Minto, C.F., Gambus, P.L., *et al.*: 'The influence of method of administration and covariates on the pharmacokinetics of Propofol in adult volunteers', *Anesthesiology*, 1998, **88**, pp. 1170–1182
- [26] Soltész, K., Dumont, G.A., van Heusden, K., *et al.*: 'Simulated mid-ranging control of Propofol and remifentanyl using EEG-measured hypnotic depth of anesthesia'. Proc. Int. Conf. 51st IEEE Conf. on Decision and Control, Maui, HI, USA, December 2012, pp. 356–361
- [27] Janda, M., Simanski, O., Bajorat, J., *et al.*: 'Clinical evaluation of a simultaneous closed-loop anaesthesia control system for depth of anaesthesia and neuromuscular blockade', *Anaesthesia*, 2011, **66**, pp. 1112–1120
- [28] Slotine, J.J.E., Li, W.: '*Applied nonlinear control*' (Prentice-Hall, NJ, 1991)
- [29] Yang, J., Li, S., Su, J., *et al.*: 'Continuous nonsingular terminal sliding mode control for systems with mismatched disturbances', *Automatica*, 2013, **49**, (7), pp. 2287–2291
- [30] Alam, W., Mehmood, A., Ali, K., *et al.*: 'Nonlinear control of a flexible joint robotic manipulator with experimental validation', *Strojniski Vestnik-J. Mech. Eng.*, 2018, **64**, (1), pp. 47–55
- [31] Ajwad, S.A., Iqbal, J., Islam, R.U., *et al.*: 'Optimal and robust control of multi DOF robotic manipulator: design and hardware realization', *Cybern. Syst.*, 2018, **49**, (1), pp. 77–93
- [32] Chaouch, S., Abdou, L., Alaoui, L.C., *et al.*: 'Optimized torque control via backstepping using genetic algorithm of induction motor', *Automatika*, 2016, **57**, (2), pp. 379–386
- [33] Ionescu, C.M., De Keyser, R., *et al.*: 'Robust predictive control strategy applied for propofol dosing using BIS as a controlled variable during anesthesia', *IEEE Trans. Biomed. Eng.*, 2008, **55**, (9), pp. 2161–2170
- [34] Noy, M.: 'Design of conical reflector to improve heating in diathermy system for palliative cancer treatment'. MS thesis, California State University, 2015